

AD-A270 387



①

WL-TR-93-7030

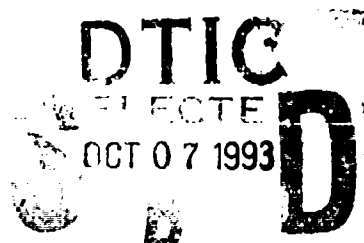
Simulating Sympathetic Detonation Effects

J. Gregory Glenn

**Wright Laboratory, Armament Directorate
Munitions Division
Energetic Materials Branch
Eglin AFB FL 32542-6810**

Mike Gunger

**Orlando Technology Incorporated
60 Second Street, Bldg. 5
Shalimar FL 32579**



SEPTEMBER 1993

FINAL REPORT FOR PERIOD APRIL 1991 - APRIL 1993

Approved for public release; distribution is unlimited.

93-23508



WRIGHT LABORATORY, ARMAMENT DIRECTORATE
Air Force Materiel Command ■ United States Air Force ■ Eglin Air Force Base

93 10 6 03 2

NOTICE

When Government drawings, specifications, or other data are used for any purpose other than in connection with a definitely Government-related procurement, the United States Government incurs no responsibility or any obligation whatsoever. The fact that the Government may have formulated or in any way supplied the said drawings, specifications, or other data, is not to be regarded by implication, or otherwise as in any manner construed, as licensing the holder, or any other person or corporation; or as conveying any rights or permission to manufacture, use, or sell any patented invention that may in any way be related thereto.

This technical report has been reviewed and is approved for publication.

The Public Affairs Office has reviewed this report, and it is releasable to the National Technical Information Service (NTIS), where it will be available to the general public, including foreign nationals.

FOR THE COMMANDER

Martin F. Zimmer

MARTIN F. ZIMMER
Technical Director
Munitions Division

Even though this report may contain special release rights held by the controlling office, please do not request copies from the Wright Laboratory, Armament Directorate. If you qualify as a recipient, release approval will be obtained from the originating activity by DTIC. Address your request for additional copies to:

Defense Technical Information Center
Cameron Station
Alexandria VA 22304-6145

If your address has changed, if you wish to be removed from our mailing list, or if your organization no longer employs the addressee, please notify WL/MNME, Eglin AFB FL 32542-6810, to help us maintain a current mailing list.

Do not return copies of this report unless contractual obligations or notice on a specific document requires that it be returned.

REPORT DOCUMENTATION PAGE			Form Approved OMB No. 0704-0188	
Public reporting burden for this collection of information is estimated to average 1 hour per response, including the time for reviewing instructions, searching existing data sources, gathering and maintaining the data needed, and completing and reviewing the collection of information. Send comments regarding this burden estimate or any other aspect of this collection of information, including suggestions for reducing this burden, to Washington Headquarters Services, Directorate for Information Operations and Reports, 1215 Jefferson Davis Highway, Suite 1204, Arlington, VA 22202-4302, and to the Office of Management and Budget, Paperwork Reduction Project (0704-0188), Washington, DC 20503				
1. AGENCY USE ONLY (Leave blank)		2. REPORT DATE September 1993		3. REPORT TYPE AND DATES COVERED Final, April 1991 - April 1993
4. TITLE AND SUBTITLE Simulating Sympathetic Detonation Effects			5. FUNDING NUMBERS C: F08630-92-R-0009 PE: 63601F PR: 670A TA: GG WU: 69	
6. AUTHOR(S) J. Gregory Glenn, WL/MNME Mike Gunger, OTI				
7. PERFORMING ORGANIZATION NAME(S) AND ADDRESS(ES) Orlando Technology Incorporated 60 Second Street, Bldg. 5 Shalimar FL 32579			8. PERFORMING ORGANIZATION REPORT NUMBER	
9. SPONSORING/MONITORING AGENCY NAME(S) AND ADDRESS(ES) Wright Laboratory, Armament Directorate Munitions Division Energetic Materials Branch (WL/MNME) Eglin AFB FL 32542-6810			10. SPONSORING/MONITORING AGENCY REPORT NUMBER WL-TR-93-7030	
11. SUPPLEMENTARY NOTES				
12a. DISTRIBUTION / AVAILABILITY STATEMENT Approved for public release; distribution is unlimited.			12b. DISTRIBUTION CODE A	
<p>13. In an effort to understand the mechanism causing sympathetic detonation, a concurrent calculational/experimental research program was initiated. The primary objective of this work was to predict the propensity of a given energetic formulation to sympathetically detonate in the storage configuration. Results from initial testing suggested the primary energy transfer mechanism associated with sympathetic detonation events involve flyer plate-like impact. To accurately describe the initial shock environment at the acceptor, accounting for pressure reduction due to divergence and donor plate thickness at impact, a simplified model was developed. It incorporated the JWL description of the donor energetic material isentrope, the unreacted Hugoniot of the acceptor energetic material, and a model derived from hydrocode analysis of the event. Donor casewall expansion velocity, peak pressure, and pulse thickness generated at casewall (flyer-plate) impact with an acceptor and divergence, and rarefaction losses were calculated. Pressure data from the impact are compared to pop plot data for the acceptor energetic material as an indicator of the materials ability to survive these conditions.</p> <p>In conjunction with the calculational effort, a flyer plate test was developed to simulate the boundary conditions found in representative donor and acceptor test configurations. Large flyer plates, 175 mm diameter by 5 to 9 mm thick, were explosively launched at velocities between 1.2 and 2.1 km/sec, which closely match the calculated casewall velocities from donor charges of interest to munitions storage problems. Runups to detonation were measured and margins of safety were determined. The insensitive materials used in these experiments were AFX-1100, a desensitized Tritonal and variations of AFX-644, mixtures of TNT, NTO, Al and wax.</p>				
14. SUBJECT TERMS JWL Equation of State, Hugoniot, MK-82, AFX-1100, AFX-644, TNT, NTO Sympathetic Detonation, Flyer Plate, Hydrocodes, Pop Plot, JWL, SDT, Flash X-ray			15. NUMBER OF PAGES 38	
			16. PRICE CODE	
17. SECURITY CLASSIFICATION OF REPORT UNCLASSIFIED	18. SECURITY CLASSIFICATION OF THIS PAGE UNCLASSIFIED	19. SECURITY CLASSIFICATION OF ABSTRACT UNCLASSIFIED	20. LIMITATION OF ABSTRACT UL	

PREFACE

This program was conducted by WL/MNME, Eglin AFB FL 32542-6810. Mr. J. Gregory Glenn managed the program. The program was conducted during the period from April 1991 to April 1993.

iii/iv (Blank)

DTIC QUALITY INSPECTED 1

Accession For	
NTIS GRA&I	<input checked="" type="checkbox"/>
DTIC TAB	<input type="checkbox"/>
Unannounced	<input type="checkbox"/>
Justification	
By	
Distribution/	
Availability Codes	
Avail and/or	
Dist	
A-1	

TABLE OF CONTENTS

Section	Title	Page
I	INTRODUCTION	1
II	SIMPLIFIED MODEL DEVELOPMENT	7
	1. Cylinder Expansion	7
	2. Impact Pressure Divergence	11
III	DEVELOPMENT OF THE EXPLOSIVELY DRIVEN FLYER PLATE TEST	17
IV	SHOCK TO DETONATION TRANSITION IN CYLINDRICAL CHARGES	25
V	EXPERIMENTAL RESULTS	27
VI	DISCUSSION AND CONCLUSIONS	29
	REFERENCES	30

LIST OF FIGURES

Figure	Title	Page
1	Typical Munition Storage Configuration.....	1
2	Hull Calculation No. 1	2
3	Hull Calculation No. 1 Showing Casewall Velocity at Impact of the Donor Casewall	2
4	Hull Calculation No. 1 Showing Pressure Pulse Inside of Acceptor Item Due to Donor Impact.....	3
5	Hull Calculation No. 2	3
6	Hull Calculation No. 2 Showing Pressure Pulse Inside of Acceptor Item Due to Donor Impact.....	4
7	Hull Calculation No. 2 Showing Casewall Velocity at Impact of the Donor Casewall	4
8	Hull Calculation of Flyer Plate With Pressure Pulse Signal Induced in the Acceptor.....	5
9	Hull Calculation of the Detonation Product Gas in Conjunction With the Flyer Plate and the Pressure Pulse Calculation for the Inside of the Acceptor Bomb	5
10	AFX-1100 Expansion Isentrope	6
11	Velocity as a Function of Volume Expansion	8
12	1-Inch Copper Cylinder Test for AFX-1100	10
13	Steel Cylinder Casewall Velocity Test Using AFX-1100	11
14	Three Impact Scenarios Using Hydrocodes	11
15	Pressure Pulse Response in the Casewall and the Explosive.....	12
16	Lagrangian Calculations of Flyer Plate Impacts.....	13
17	Sphere Impacting a Plane Surface	13
18	Geometry Used to Describe Equation 19.....	14
19	Plot of AFX-1100 Side-By-Side Impact Scenario at Various Expansions.....	16
20	Hydrocode Calculation of Thin-Walled Cylinder.....	17
21	Hydrocode Calculation of Thick-Walled Cylinder	18
22	Energetic Materials Branch Flyer Plate System	19
23	Top View of the Flyer Plate Test Setup.....	20

LIST OF FIGURES (Concluded)

Figure	Title	Page
24	Side View of the Flyer Plate Test Setup	20
25	Hydrocode Calculation Predicting High Pressure Region on Edges of Plate	21
26	Flash X-Ray of the Flyer Plate Showing High Pressure on Edges of Plate.....	21
27	Edge Effects Elimination Device.....	22
28	Hull Calculation With Flyer Plate Not in Contact With Steel Cylinder.....	22
29	New Flyer Plate Launch System for Low Velocity Plates	23
30	Flash X-Ray of Flyer Plate With Uniform Pressure Distribution Across Back Surface of Plate	23
31	AFX-6441 Calculation of the Detonation of the Donor Bomb With a Flyer Plate Forming at 75 μ s	23
32	Plot of Flyer Velocity Versus Explosive Thickness.....	24
33	Flyer/Acceptor Setup With Pins in Place	25
34	Side View of the Flyer/Acceptor Setup.....	25
35	Overall Test Setup.....	26
36	Comparison of the Simplified Model With the Experimental Data.....	27
37	Manganin Gauge Data	28

SECTION I

INTRODUCTION

Suppression of sympathetic detonation between stored munitions has been a very important issue in the 1990s for all branches of the Department of Defense.

During the Air Force's Insensitive High Explosives (IHE) development program, a series of live typical munition storage items in a standard storage configuration was tested using AFX-1100, TNT/wax/Al (66/15/18 percent by weight). The storage configuration is shown in Figure 1. For symmetry and worst case conditions, the donor was placed in the bottom middle position. It was found that the left and right bottom and top center items did not detonate when exposed to the detonation of the donor. It was also observed that the left and right diagonal items consistently detonated. Since the items did not detonate in a side by side test at the same diagonal distance, it was hypothesized that the confinement of the donor item due to the top center, bottom left and right items was causing an enhancement of the munition case velocity up to the critical initiation pressure of AFX-1100 for items located in the diagonal position.

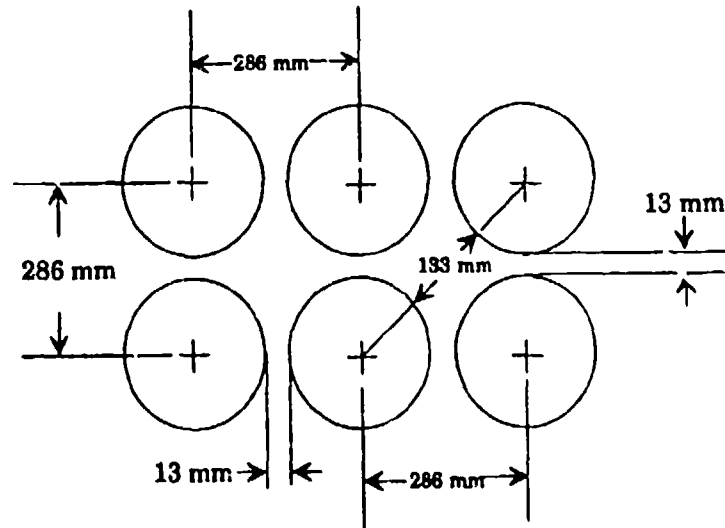


Figure 1. Typical Munition Storage Configuration

A second series of tests was conducted to verify the hypothesis. The tests were designed to alleviate some of the confinement of the donor by elevating the top row of munition items. The minimum separation distance for the munition case was 13 mm horizontally and vertically. The diagonal distance was 133 mm. As the top row of items were moved up, which reduced the confinement, the diagonal item no longer sustained a detonation. It appeared that the hypothesis was true. But upon further investigation using hydrocodes (Reference 1) it was determined that the casewall of the donor item, with the top row of items elevated, produced a higher velocity during the detonation than did the standard confinement case. Figure 2 is a hull calculation 100 μ s into the detonation of the donor with the items in the normal stacking configuration. Figures 3 and 4 are time history data of donor casewall velocity and acceptor pressure for this calculation.

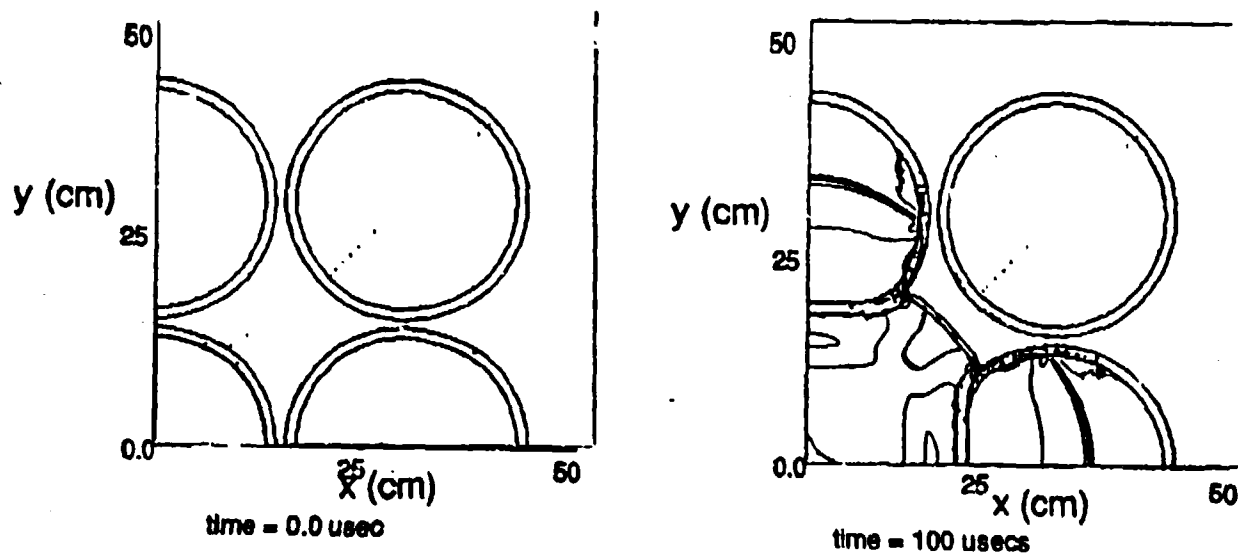


Figure 2. Hull Calculation No.1

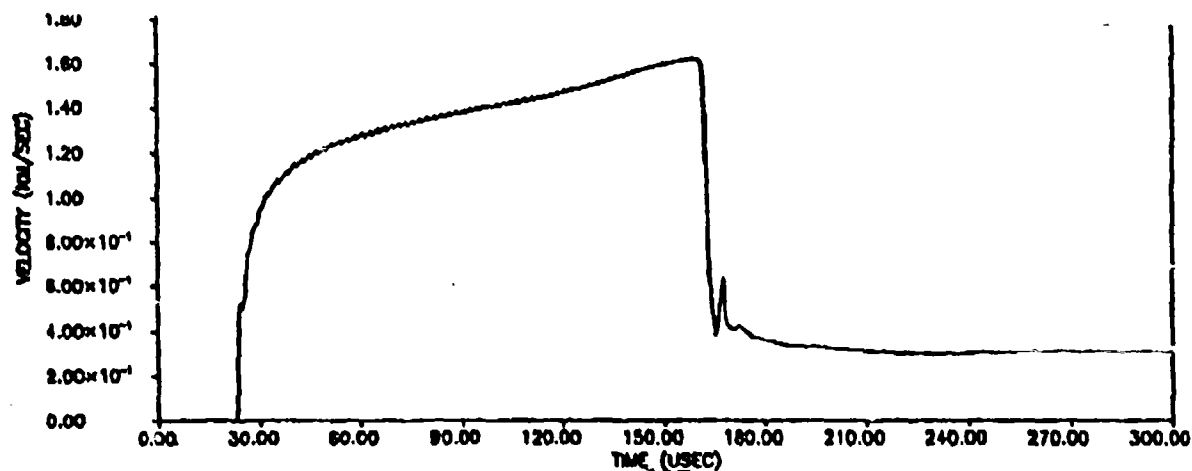


Figure 3. Hull Calculation No.1 Showing Casewall Velocity at Impact of the Donor Casewall

Notice that the flyer casewall velocity for the standard configuration case was 1.55 mm/ μ s and the pressure induced inside the acceptor explosive was 55 kbars. By way of comparison, the critical initiation pressure for AFX-1100 as measured by the modified Expanded Large-Scale Gap Test (ELSGT) is between 53 and 56 kbars. The ELSGT pulse duration is very similar to that calculated for the diagonal item shown in Figure 2. Thus because the calculation predicts that the diagonal item is at the initiation threshold for AFX-1100, we should expect the acceptor to detonate.

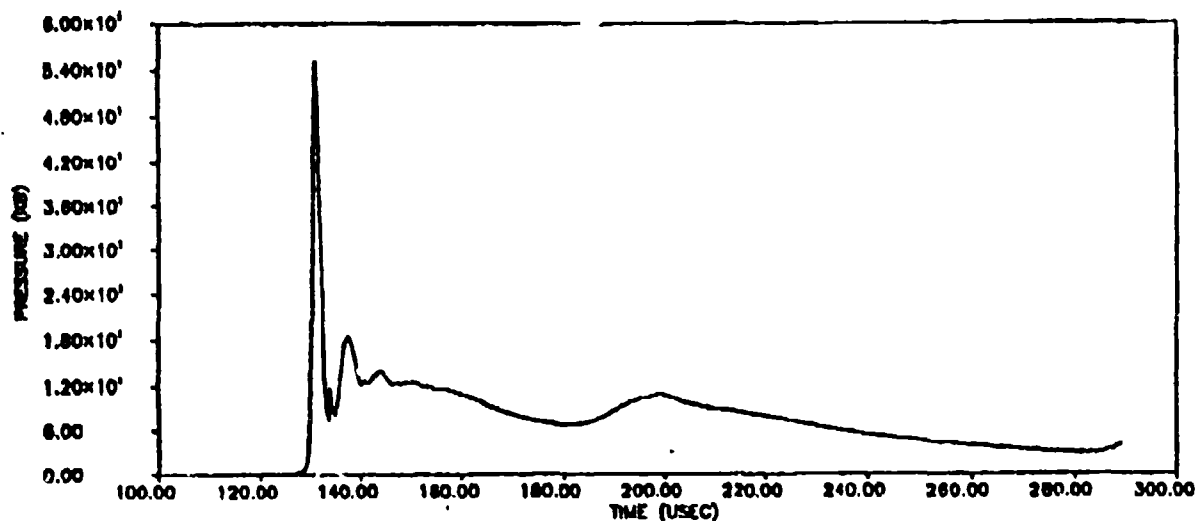


Figure 4. Hull Calculation No.1 Showing Pressure Pulse Inside of Acceptor Item Due to Donor Impact

The next series of calculations were performed at a non-detonating height for the diagonal item of 76 mm as measured vertically on the outside of the items. Notice in Figure 5 that at 100 μ s the flat plate generated from the donor casewall appears to have thinned more than in the previous test (see Figure 2). Thinning of the casewall is directly related to the amount of expansion the munition case is allowed to undergo. As a general rule it is assumed that the munition case will expand up to two times the initial radius before it breaks up. In Figure 6 the pressure induced inside the acceptor item is calculated to be 44.6 kbars, approximately 10 kbars below critical initiation pressure. The velocity of the thinned casewall at impact on the diagonal acceptor item is 1.62 mm/ μ s as shown in Figure 7. The calculation predicts no initiation in this instance and is consistent with the experimental observation.

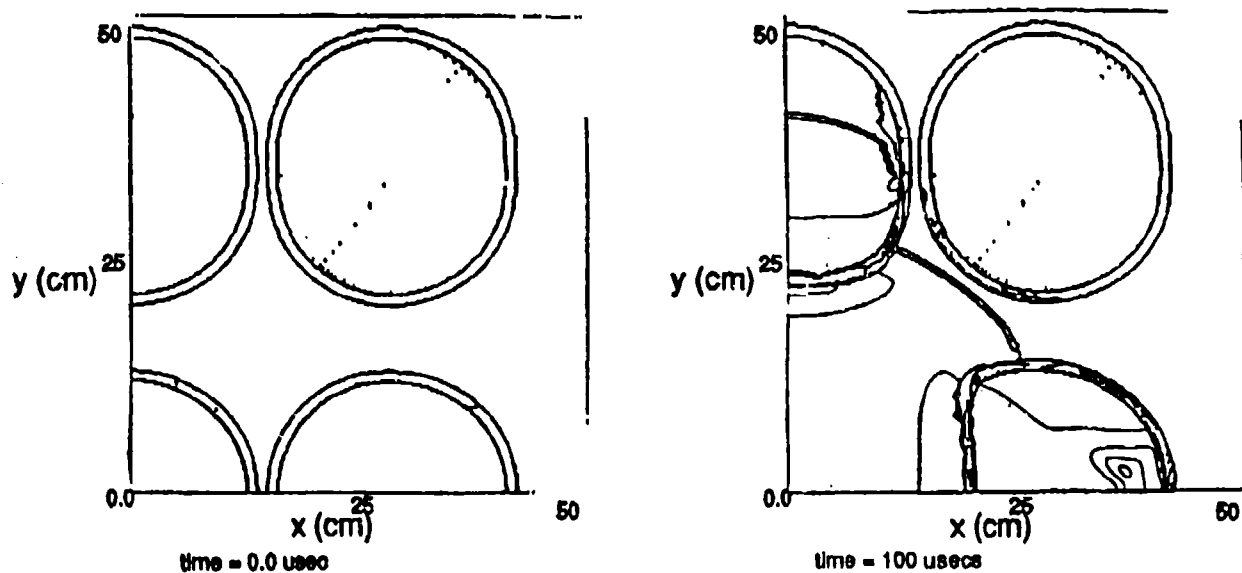


Figure 5. Hull Calculation No. 2

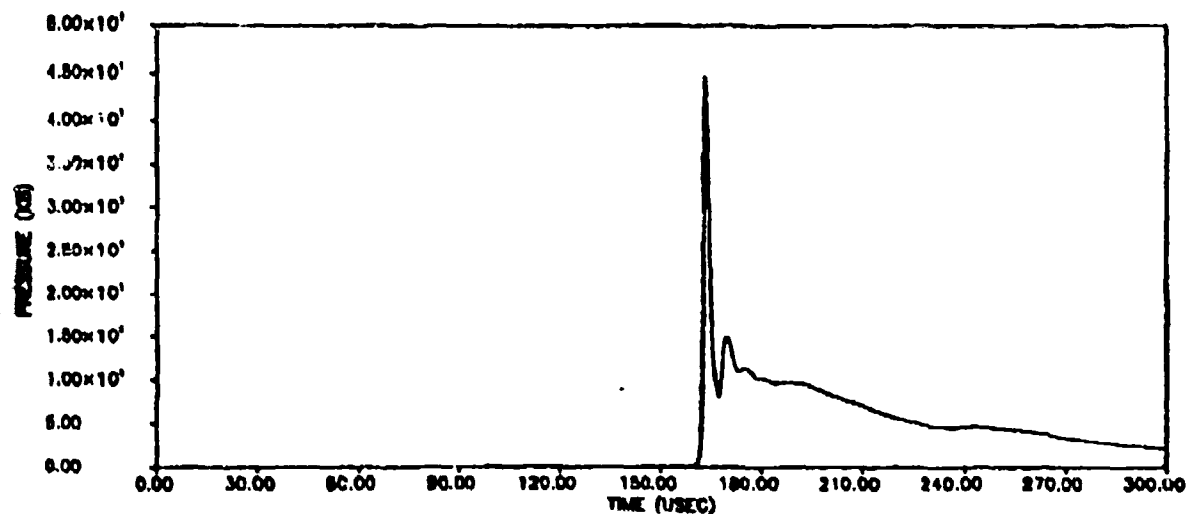


Figure 6. Hull Calculation No.2 Showing Pressure Pulse Inside of Acceptor Item Due to Donor Impact

As the top row of bombs is raised, the donor casewall expands further, hence thins more, prior to impact with the center item of the top row. Although confinement does not result in higher case velocity, it does reduce case thinning given the case is not free to expand radially.

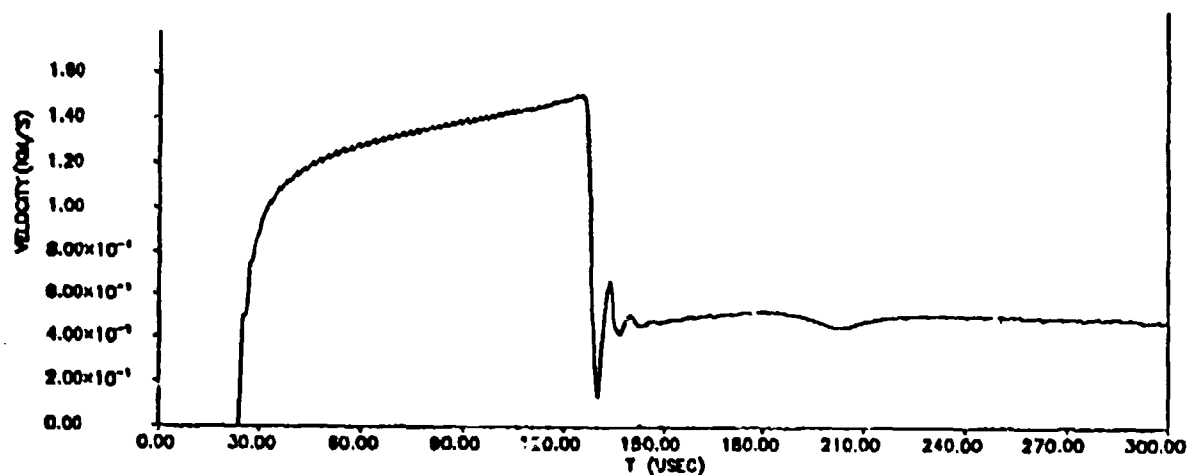


Figure 7. Hull Calculation No. 2 Showing Casewall Velocity at Impact of the Donor Casewall

A calculation was also performed to determine if the complex geometry depicted in Figure 2 could be modeled by impacting a single cylinder with a fiat plate as shown in Figure 8. The pressure observed at the first unmixed cell was 55.7 kbar; recall that the pressure predicted for condition in Figure 2 was 55 kbar.

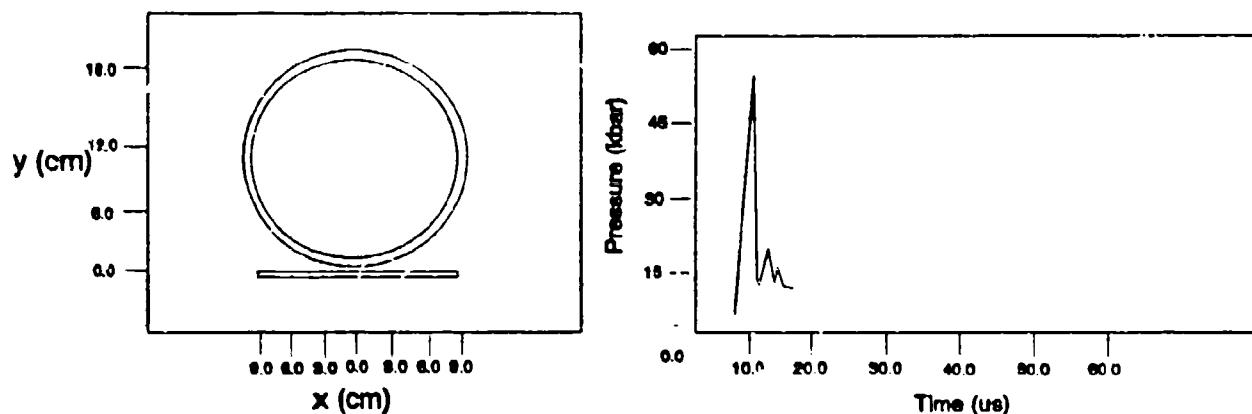


Figure 8. Hull Calculation of Flyer Plate With Pressure Pulse Signal Induced in the Acceptor

The next calculation was performed to see if the detonation products contributed to the overall energy of the flyer plate. We have hypothesized that the munition test as shown in Figure 1 is a long impulse event. However, from Figure 4, very little area exists under the initial pressure pulse. This implies that the pressure duration is controlled by the thickness of the impacting casewalls with little contribution from the detonation products. Based on the calculation of the detonating donor item, at impact, the gases have expanded into a volume V/V_0 of between 2 and 3. A complete history of the expansion isentrope of the donor item is shown in Figure 10. The pressure associated with this expansion is between 2 and 5 kbars. To verify that the pressure behind the flyer plate was not contributing to the input pressure as seen by the acceptor explosive, a calculation shown in Figure 9 was performed with 10 kbars of pressure behind the flyer plate. All the other conditions were kept the same. The pressure at the first unmixed cell inside the acceptor case was 58 kbars. It is apparent that the contribution of the product gases to the input pressure is minimal. Based upon all of the information, it is believed the diagonal acceptor is being initiated by a shock to detonation transition that is directly related to the velocity, thickness, and shape of the flyer plate. From this information the Explosively Driven Flyer Plate Test was developed to reproduce the boundary conditions as observed with experiment and hydrocode calculations.

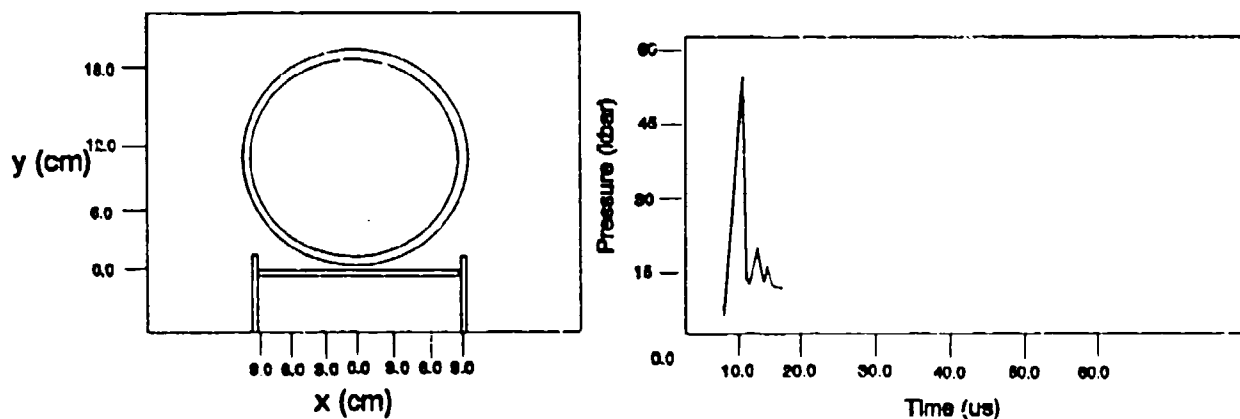


Figure 9. Hull Calculation of the Detonation Product Gas in Conjunction With the Flyer Plate and the Pressure Pulse Calculation for the Inside of the Acceptor Bomb

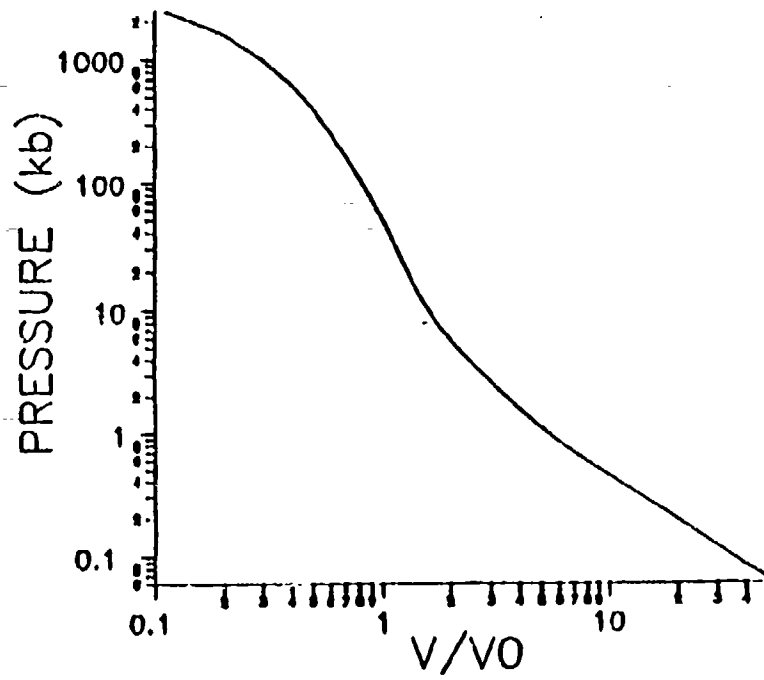


Figure 10. AFX-1100 Expansion Isentrope

SECTION II

SIMPLIFIED MODEL DEVELOPMENT

The development of a simplified model to predict the results of the flyer plate test was considered essential for numerous reasons. Principally, if the event was well understood, a model could be developed and also, with a simplified model, the necessity of understanding both the equations of state and numerical methods employed in a large, multimaterial, multidimensional finite difference code, such as the OTI*HULL code, could be avoided. This is particularly true of resolution requirements that in a simplified model can be avoided altogether. For the development and checkout of the model, the OTI*HULL code was used.

The model is broken into three parts: (1) the cylinder expansion, (2) impact, casewall pressure divergence, and (3) the acceptor explosive evaluation. Each of these parts will be addressed separately.

1. CYLINDER EXPANSION

The model currently allows the user three separate means of determining the donor casewall impact velocity. The first method is a straightforward integration of the expansion isentrope. The second method attempts to better match cylinder expansion data through the use of impulse momentum. The last is a combination of the first two methods. The Jones, Wilkins, and Lee (JWL) description of the expansion isentrope is

$$P = ae^{-r_1 v} + be^{-r_2 v} + c_1 v^{-(w+1)} \quad (1)$$

where a, b, c, r_1 , and r_2 are constants which allow for a non-constant γ and V which is the ratio of V/V_0

The integration of the expansion isentrope can be found in numerous references but for this application the method given by Miller (Reference 2) in Equation 1 is most suitable. To avoid repetition, only a summary will be given here. The energy as a result of Pdv work is written as:

$$\int_{E_0}^E dE = \int_1^V p dV \quad (2)$$

or

$$E = E(V=1) - \left(\frac{a}{r_1} e^{-r_1 v} + \frac{b}{r_2} e^{-r_2 v} + \frac{c}{w} V^{-w} \right). \quad (3)$$

From the Gurney relation,

$$Eg = E_0 \left(\frac{M}{V} \right) \left(1 + 0.5 \rho / \frac{M}{V} \right) \quad (4)$$

$$v = \sqrt{2Eg}.$$

Then setting $E(V=1)$ equal to the heat of detonation, the energy given by Equation 3 can then be substituted into Equation 4 for E_{19} giving the velocity as a function of volume expansion.

A plot using this method can be seen in Figure 11 with a hydrocode calculation also shown for comparison. Late time data is fit very well but early time response, which is controlled by momentum transfer, is not.

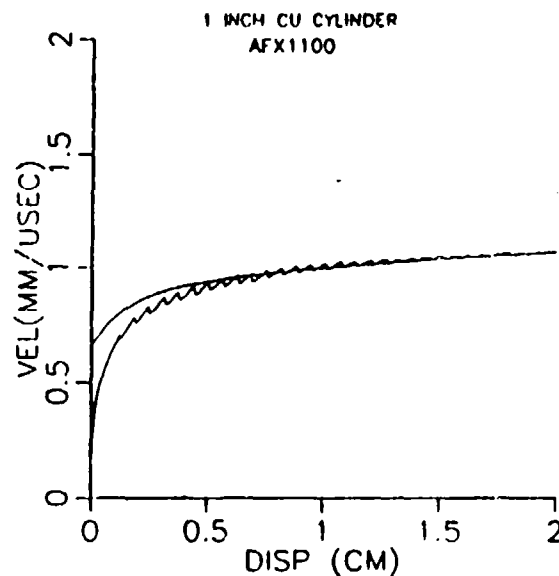


Figure 11. Velocity as a Function of Volume Expansion

To overcome this difficulty, a model based upon impulse and momentum as given by Equation 5 was developed.

$$\int F dt = \int M dv \quad (5)$$

where

F = force
 dt = loading duration
 M = mass
 dv = change in velocity.

Substituting the pressure, inside casewall area and mass into Equation 5 yields:

$$v_i = v_{i-1} + \frac{PA_{i-1}dt}{M} \quad (6)$$

A_{i-1} = Area of the inside casewall

Since this equation by itself does not yield a unique result, all quantities are scaled to the 1-inch copper cylinder test. The equations are cast in plane geometry so that dt is taken as the transit time of the detonation wave over 1 cm (10 mm). This result is further broken down into n divisions. Further, the initial casewall volume ($V/V_0 = 1$) which implies that the Chapman Jouget (CJ) pressure is never attained. To avoid this difficulty, the CJ volume is calculated as Equation 7:

$$V_j = \frac{\gamma}{\gamma + 1} V_o. \quad (7)$$

This value is subtracted from the initial volume ratio (1) so that the volume ratio input to the JWL equation of state (EOS) is reduced for a time by this amount. However, once the reaction zone passes a given part of the cylinder, this volume reduction no longer applies. It is assumed that when the shock wave reaches the cylinder free surface, this volume reduction is removed. To calculate the shock velocity in the casewall due to the impact of a detonation wave, Equation 8 is applied.

$$\left[\frac{u_1 - u}{\gamma D / (\gamma + 1)} \right]^2 = \frac{2}{\gamma(\gamma + 1)} \frac{(P / P_1 - 1)^2}{P / P_1 + (\gamma - 1) / (\gamma + 1)} \quad (8)$$

where u_1, P_1, D, γ refer to the CJ condition.
 u = particle velocity, P = pressure, D = detonation velocity.

The intersection of Equation 8 with the casewall Hugoniot provides the interface particle velocity. Substitution of the interface particle velocity into the casewall Hugoniot provides the shock velocity in the casewall.

Knowing the time step (divided by n divisions), the number of required iterations can be calculated as:

$$\text{Iter} = (\text{cwt} / U_{s_c})(n / \text{dcji}) \quad (9)$$

where

cwt = casewall thickness
 U_{s_c} = shock velocity in casewall
 n = number of divisions
 dcji = detonation velocity of explosive.

Since the equations are cast in plane geometry, only radial expansion can be considered. However, it has been found necessary to allow the volume to expand axially as a function of the particle velocity. This can be expressed as:

$$h = h_{i-1} + U_p * k \quad (10)$$

The particle velocity (U_p) can be calculated from the momentum equation as:

$$U_p = P / \rho_o U_s \quad (11)$$

where ρ_o is the ambient casewall density

The shock velocity, U_s , is given as Equation 12.

$$U_s = \sqrt{\frac{P * (\gamma + 1)}{\rho_o}} \quad (12)$$

The variable γ can be calculated from the JWL EOS as:

$$\gamma = \frac{v(r_1 a e^{-R_1 v} + r_2 b e^{-R_2 v} + c(w+1)v^{-(w+2)})}{a e^{-R_1 v} + b e^{-R_2 v} + c v^{-(w+1)}} \quad (13)$$

To match the cylinder expansion with a minimum number of time steps, the interface pressure may also be applied for a short duration but not exceeding the number of iterations given by Equation 10.

With these equations, the casewall expansion, hence volume increase, can be calculated from Equation 6. The number of divisions (n) and the axial expansion constant k are determined from 1-inch copper cylinder test results (or hydrocode calculations). Both constants are varied until the calculated cylinder test matches the experimental results. Values for n vary between 10 and 30 and is essentially controlled by the explosive energy. Generally, the more energetic the explosive the more divisions required. The axial expansion constant is usually between 0.1 and 0.2. Calculations performed at other charge to mass ratios are scaled to the 1-inch cylinder results. The axial expansion constant is given as:

$$k = (1 - cm_r + xp)(r_r) \quad (14)$$

where cm_r = ratio of charge to mass of a 1-inch copper cylinder of the same explosive to the ratio of the current casewall material to explosive

xp = axial expansion constant for one copper cylinder

r_r = ratio of current inside radius to inside radius of a one inch copper cylinder.

Note that this term reduces to zero for the 1-inch test with no axial expansion (xp). Values for the axial expansion constant are generally in the range of 0.1 to 0.2 for the 1-inch test. Results for this model are shown in Figures 12 and 13 with the first being a copper cylinder test and the second a steel cylinder with a cross section corresponding to a general purpose bomb.

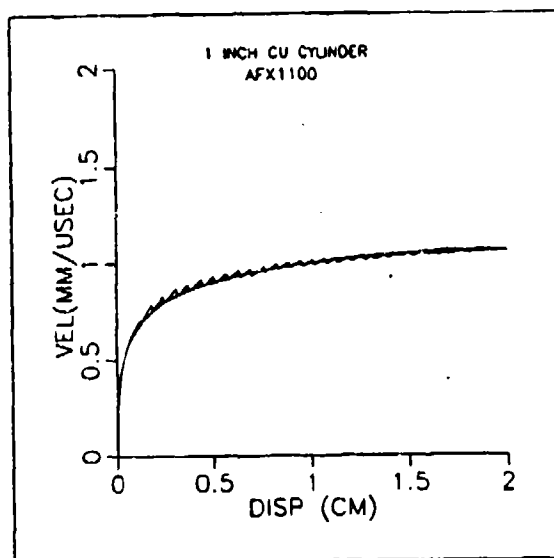


Figure 12. 1-inch Copper Cylinder Test for AFX-1100

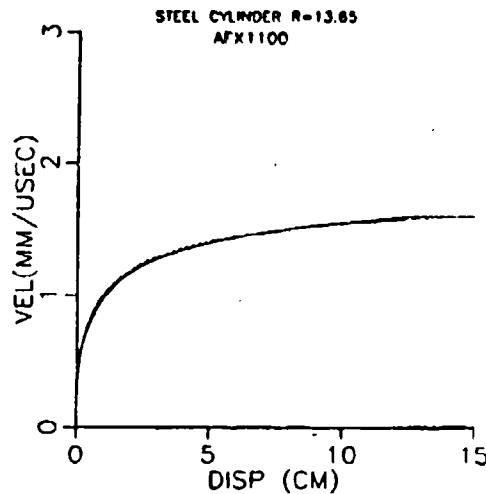


Figure 13. Steel Cylinder Casewall Velocity Test Using AFX-1100

Velocities are limited to the Gurney velocity. At a volume ratio of approximately 2, the impulse-momentum calculation can be terminated and the remaining expansion calculated as a function of energy. This method is preferred since the energy method is significantly faster and produces better late time results. The casewall motion as a function of displacement is now determined. The casewall thickness as a function of expanding radius can be calculated through the continuity equation as:

$$t_{cu} = r - \sqrt{r_i^2 - r_o^2 + r^2} \quad (15)$$

where

r = the current radius

r_i = initial inside radius

r_o = initial outside radius.

2. IMPACT PRESSURE DIVERGENCE

The results of the previous section indicate the impact velocity can be calculated to within a few percent. From the impact velocity, the initial pressure in the casewall can be determined. Without divergence, that pressure will be uniform throughout the material thickness. However, through hydrocode analysis, a significant amount of pressure divergence can be observed in the casewall. Figure 14 depicts the results of three impact scenarios involving a purely one-dimensional flat plate impact, a flat plate impacting a right circular cylinder, and a curved plate impacting a right circular cylinder.

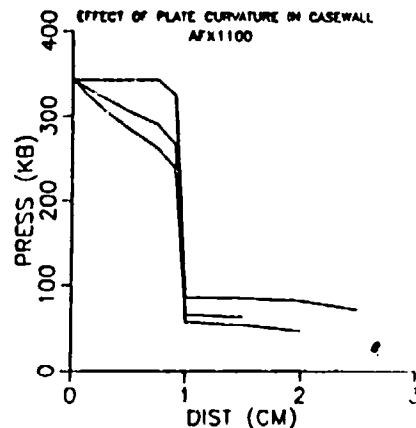


Figure 14. Three Impact Scenarios Using Hydrocodes

The pressure pulse response in the casewall and in the explosive can be seen in Figure 15. Note that the pulse duration is the same for all three cases.

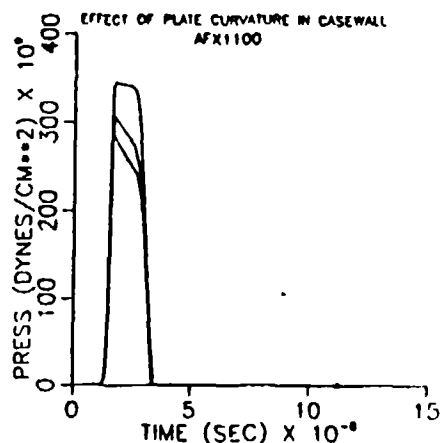


Figure 15. Pressure Pulse Response in the Casewall and the Explosive

These calculations were performed using the lagrange module in OTI*HULL at a resolution required to predict the analytical one-dimensional flat plate pressure. The ratio of impacting plate thickness to acceptor plate is 0.5. The impacting velocity is 1.5 mm/usec. As can be seen, each case begins at the same initial pressure, which can be calculated through the momentum equation and material Hugoniot. The one-dimensional momentum equation is written as:

$$P = \rho_0 U_s U_p \quad (16)$$

where

ρ_0 is the initial density
 U_s is the shock velocity
 U_p is the particle velocity.

For most solid materials, the shock velocity can be related to the particle velocity at the linearly as:

$$U_s = C + S U_p \quad (17)$$

where

C is the ambient longitudinal sound speed
 S is the Hugoniot slope.

For like materials, the interface pressure at impact can be expressed as:

$$P = (\rho_0/2)(U_p/2)(C + S U_p/2). \quad (18)$$

For dissimilar materials, a reflected Hugoniot is employed. The particle velocity at the interface in the receiving material can be expressed as:

$$U_p = 2U_1 - U. \quad (19)$$

The unsubscripted variables represent the interface conditions. Equations 16 and 19 can then be written on both sides of the interface and the resulting interface particle velocity solved for, which in turn provides the interface pressure. Figure 16 depicts two impact scenarios involving different plate thicknesses and impact velocities.

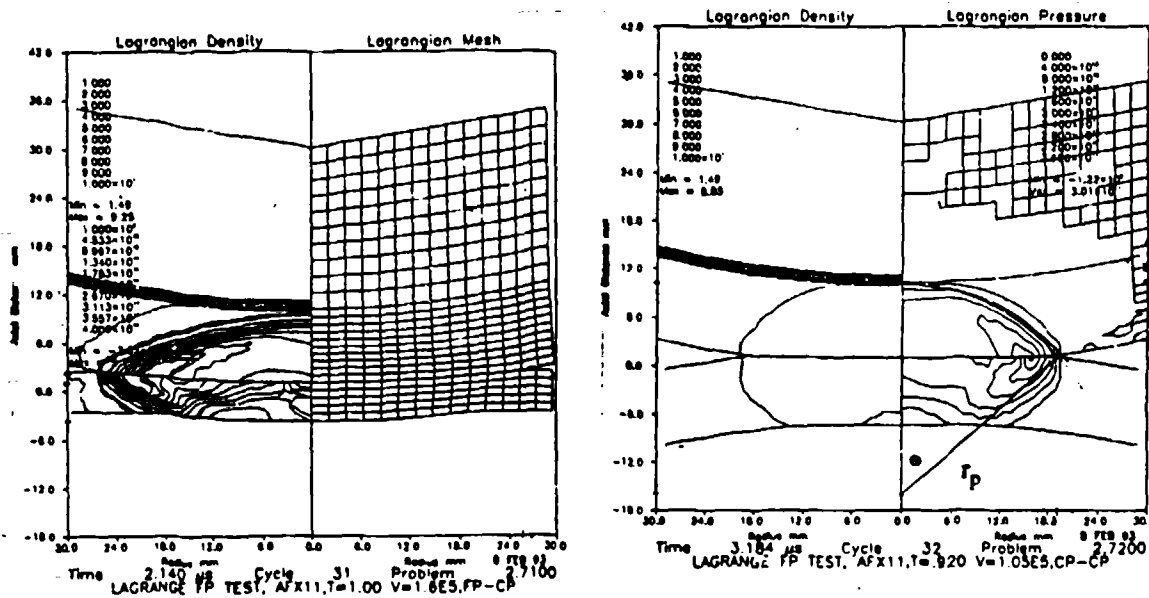


Figure 16. Lagrangian Calculations of Flyer Plate Impacts

Note the radius of curvature of the resulting pressure wave due to the impact. Essentially, the wave begins at the impact point and terminates at the end of the impacting plate. The magnitude of the initial shock wave pulse can be reduced in two ways: either through wave divergence or rarefactions resulting from free surface interaction. The problem then is to determine the minimum diameter equivalent plate that reproduces the conditions involved in the original impact problem. Work involving spherical fragments (Reference 3) indicated that the equivalent flat plate was controlled by lateral free surface relief that occurred when the plate closing rate was exceeded by the velocity of rarefaction waves, which were set equal to the ambient sound speed in the material. Since the spheres were solid, a one-dimensional region was considered to exist in the impacted material prior to relief due to the rarefaction waves. For a sphere impacting a plane surface, as shown in Figure 17, with time referenced to the center of the sphere, the equivalent plate diameter was given as:

$$d_i = 2y(1 + Co^2/u_i^2) \cdot 5 \quad (20)$$

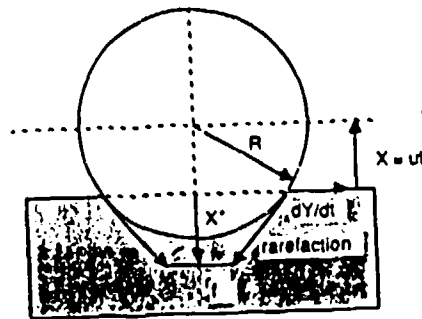


Figure 17. Sphere Impacting a Plane Surface

The geometry of the event is shown in Figure 18. Victor (Reference 4) extended this to curved plates with the equivalent plate given as:

$$d_i = 2r_a(v_r/Co_c)(r_d + L)/(r_a + r_d + L) \quad (21)$$

where

- r_a is the radius of the acceptor
- v_r is the velocity at donor radius r
- r_d is the initial donor radius
- L is the shortest distance between donor and acceptor.

Work performed by Green (Reference 5) suggested that lateral rarefactions enter into the one-dimensional region from 45 degree angles. Therefore if the lateral extent was known, propensity toward sympathetic detonation could be determined by examining the depth into the explosive the one-dimensional region extended and comparing that value to the explosive critical diameter. For depths less than the critical diameter, an expanding wave approximation of the form (Equation 22) could be used.

$$P_{eqv} = P_o \left[\frac{1}{1 + \sqrt{2} \left(\frac{x_i}{d_o} \right)} \right] \quad (22)$$

where

x_i is the distance into the acceptor
 d_o is the equivalent flat plate diameter.

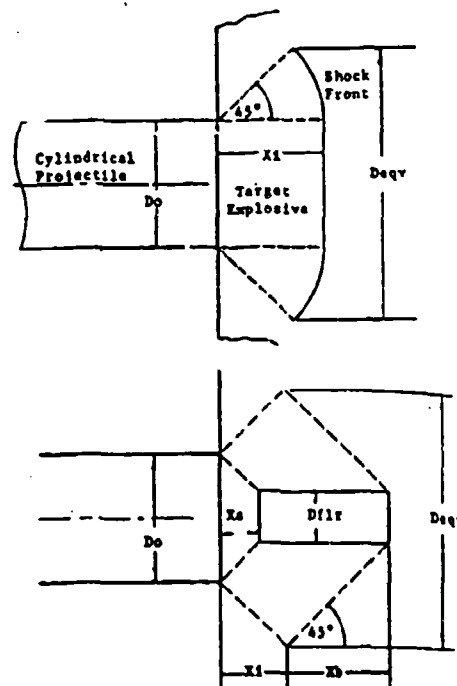


Figure 18. Geometry Used to Describe Equation 19

As mentioned previously, considerable divergence exists within the casewall and must be taken into account. In addition, rarefactions also enter due to rear surface relief and may control the plate diameter. Hydrocode results suggests that a better approximation to the equivalent flat plate can be determined by replacing the ambient sound speed in either Equations 20 or 21 with the shock velocity appropriate to the impact velocity determined through the momentum equation. This result is then compared to the plate diameter calculated assuming rear surface relief is the controlling mechanism. An initial approximation of the available time is made by determining the transit time of a shock wave across the acceptor thickness. This time is compared to the time of a rearward propagating shock wave into the donor plate. The donor plate rear surface continues at the initial impact velocity until encountering the rearward propagating shock wave.

This determines both the plate thickness and pulse duration into the explosive. This time can be expressed by:

$$t = \text{plate thickness} / (\text{impact velocity} + \text{shock velocity}) \quad (23)$$

The surface then moves

$$rsm = t * v \quad (24)$$

where v = impact velocity, and rsm = rear surface movement.

The new plate thickness is then

$$T_{pln} = T_p - rsm \quad (25)$$

where the old plate thickness T_p is calculated through the continuity equation as:

$$tp = r_{o2} - \sqrt{r_{o2}^2 - (r_{o0}^2 - r_{i0}^2)}$$

where r_{o2} is the outside radius at impact
 r_{o0} is the initial outside radius
 r_{i0} is the initial inside radius.

Initial efforts to determine the extent of pressure divergence centered on a modified cylindrical expansion of the pressure. Essentially, the wave was allowed to expand at the shock velocity induced by the impacting plate until the shock wave at the centerline encountered the casewall/explosive interface. A circle was then fit to the centerline explosive/casewall interface and the radial (x,y) position of the plate. The force was then assumed to expand to the arc length given in this fashion. This can be expressed as:

$$P_{eqv} = P_o * (\text{arclng}/d_i) \quad (26)$$

where d_i is the radial extent of the shock wave (equivalent plate radius).

However, the interface pressures calculated in this fashion were high relative to the hydrocode calculations. A better approximation and the one currently in use is given as:

$$P_{eqv} = P_o * (\cos \xi / r_p) \quad (27)$$

where r_p is the radius of the pressure pulse. As the impact becomes more one dimensional, the pulse radius becomes large. Since the plate diameter is limited to the radius of the acceptor round, hence finite, the interface pressure approaches the impacting pressure. The solution is actually performed in two iterations. With the pressure calculated at the interface, a new shock velocity can be calculated. Because this velocity is calculated, a new available time is determined. Figure 19 is a plot of an AFX-1100 loaded MK-82 in a side-by-side impact scenario at various expansions. The pressures plotted were calculated in the explosive using both the OTI*HULL code and Equation 27.

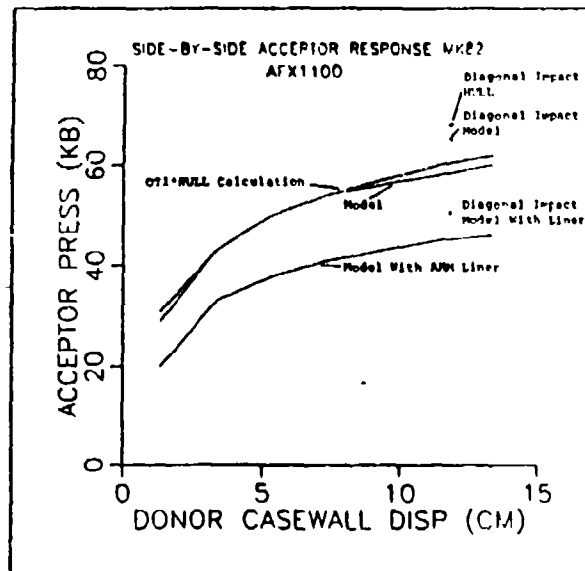


Figure 19. Plot of AFX-1100 Side-By-Side Impact Scenario at Various Expansions

Included in the model is the ability to insert a liner in the casewall. Again, Figure 19 shows the results of including the liner. It is interesting to note that without the liner, donor casewall expansions greater than 3.5 cm produced detonations in side-by-side impact calculations involving AFX-1100 explosive. Tests of this same event produced no detonation in side-by-side configurations. With the addition of the 2.5 mm thick liner, the model recreated the test results. In addition, the pressures so calculated were almost identical to previous coarsely zoned calculations without a liner that also reproduced the test results. For small expansions, the isentrope pressure may be significant. This pressure is added such that the total interface pressure is given as:

$$P = P_{eqv} + P_{jwl} \quad (28)$$

The assumption is that the isentrope pressure pulse duration at the peak is of the order of the reaction zone length, which is of almost zero duration relative to the case pulse. The pressure pulse is then triangular with a duration at the base given by Equation 23.

The hydrocode results indicate that for the pulse controlled by the plate thickness, a one-dimensional region in the explosive does exist primarily due to the shock velocity difference between the undetonated explosive and the metal casewall. After this region, the expanding wave equation by Green provides good results.

With the peak pressure and duration in the explosive determined, the likelihood of sympathetic detonation can be determined in many ways. The model currently uses the critical diameter method to evaluate sympathetic detonation. If the minimum go pressure recorded in the wedge test extends beyond the critical diameter of the wedge test, a go is assumed.

SECTION III

DEVELOPMENT OF THE EXPLOSIVELY DRIVEN FLYER PLATE TEST

Information provided in Reference 6 was used to devise a method for accelerating and launching flyer plates into explosive targets. Through hydrocode analysis and test constraints, the most feasible configuration consisted of a plate 180 mm in diameter with a thickness up to 12.7 mm. In order to recreate the boundary conditions observed in the pallet test, the velocity range would be between 1.4 and 2.2 km/sec.

The basic requirement consists of using thick walled cylinders greater than 76 mm thick to ensure shock wave rarefactions from the free surface do not interfere with the plate acceleration. In addition, the pressure distribution across the plate face must be as uniform as possible to prevent distortion. During the detonation process the center of the explosive is the highest pressure region. Therefore the head height of the explosive is important in determining the flatness of the plate. If the length of the charge is too short, the detonation wave will be very curved. If this wave impacts the plate, the plate will be bent accordingly. Another technique that is used to produce a flat plate is the use of an air gap between the explosive and the flyer plate. If the detonation wave is very curved when it moves into the air gap, it immediately slows down but the edges of the detonation wave are still traveling at the detonation velocity of the explosive. Therefore they catch up to the shock front, and the wave that impacts the plate is now flat. Figure 20 is a hydrocode calculation demonstrating what happens to a flyer plate when these techniques are not applied. For this particular calculation the casewall of the cylinder is very thin, 13 mm, and there is no air gap between the plate and the explosive. Notice the curvature of the flyer plate.

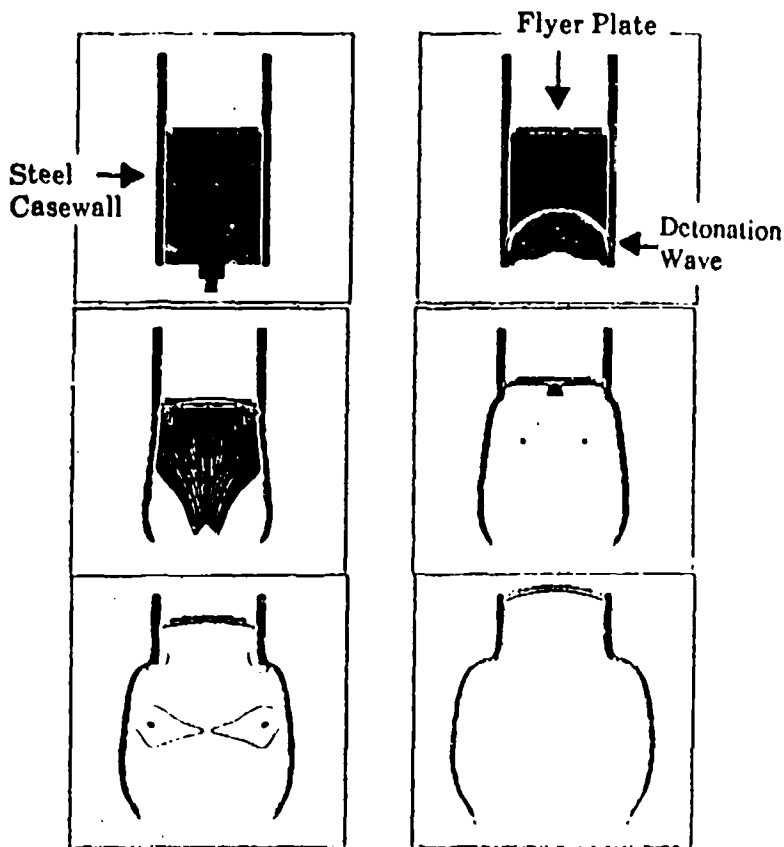


Figure 20. Hydrocode Calculation of Thin-Walled Cylinder

Hydrocodes were used extensively in the development of the flyer plate test. They helped to identify all aspects of the detonation/shock wave interaction and allowed a look at different combinations of air gap, head height, and flyer plate thickness.

Figure 21 is a hydrocode calculation showing the benefits of having a thick cylinder 50 mm wall thickness and an air gap between the explosive and the flyer plate. Notice the flatness of the flyer plate.

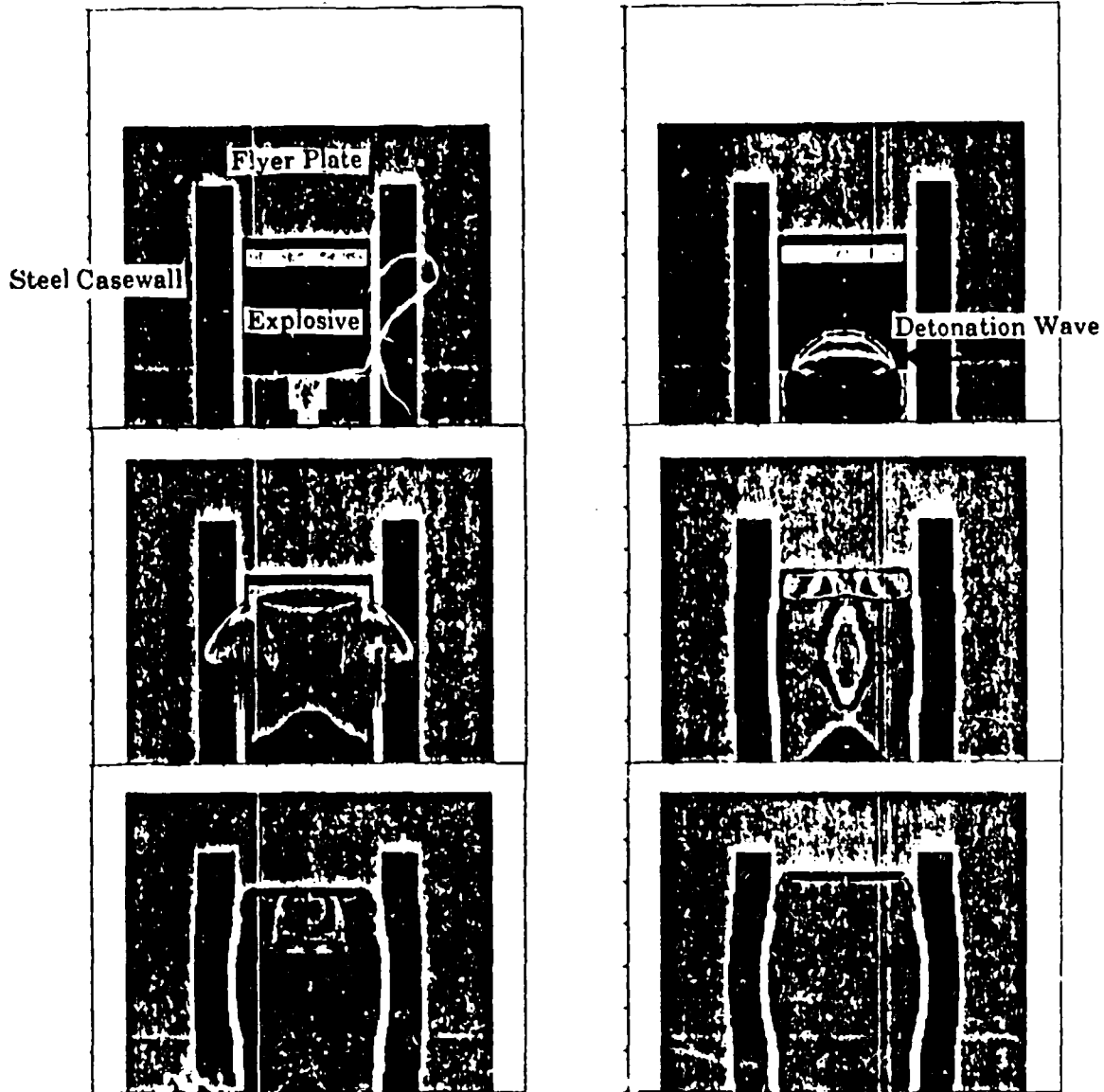


Figure 21. Hydrocode Calculation of Thick-Walled Cylinder

The explosive that was used to launch the flyer plates was AFX-1100; it consists of TNT, wax, Al (66/16/18 percent by weight). It was picked because it had a low detonation pressure 125 kbars, which would help prevent spall from occurring from the flyer plate. Pentolite was used as a booster to avoid overdriving the AFX-1100 main charge. The detonation train consists of a 50 x 25 mm pentolite booster, 25 x 25 mm A-5 pellet, and an RP-83 detonator.

For the test setup the flyer plate was epoxied into a 250 mm long by 200 mm diameter steel cylinder that had a casewall thickness of 13 mm. The air gap device is placed first behind the flyer plate and then the explosive. With the small can loaded, the next step is to place it into a larger (400 mm long by 300 mm outside diameter with a 50 mm wall thickness) steel cylinder. By having the smaller steel cylinder already loaded, it greatly simplifies and prevents alignment error from occurring during the assembly at the range. The face of the flyer plate in the small cylinder should be placed 76 mm from the end of the bigger steel cylinder. This distance, 76 mm, was a compromise; it was a trade-off between having the plate too far back into the barrel, which would cause damage to the plate from the product gases, or too far out with no contribution from the product gases at all. Figure 22 shows the system now being used. The flyer plate, explosive, air gap device and steel cylinders have all been precision machined to ± 0.127 mm for a form fit.

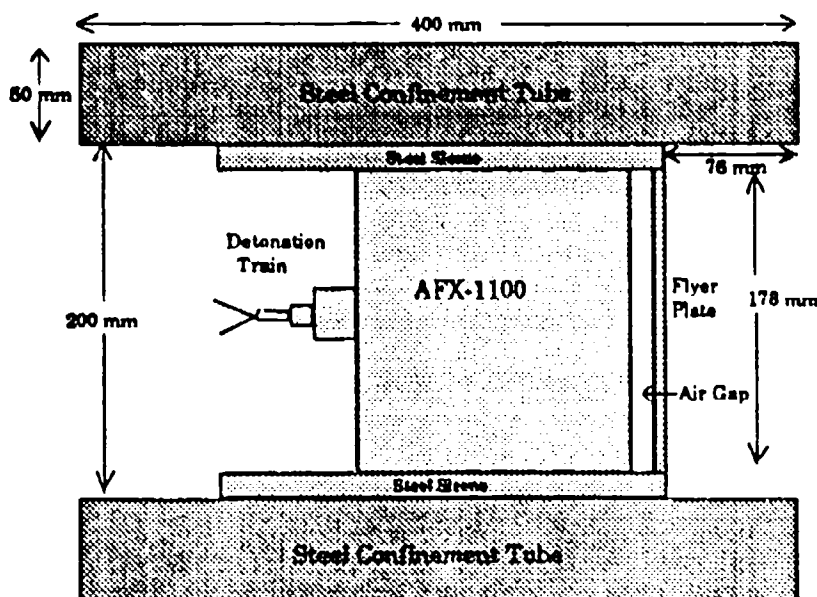


Figure 22. Energetic Materials Branch Flyer Plate System

The thickness of the flyer plate has been found to be a very critical element in determining the pressure induced inside the acceptor charge. The proper thickness of the flyer plate was determined by hydrocode calculations and measurement of post-test bomb fragments. Both the hydrocodes and the post-test data verified that the fragments had thinned down from 10 to 6 mm. Therefore the flyer plate thickness that will be used for this investigation will be 6 mm. The main method for acquiring plate velocity and integrity data is flash radiography. This method is used to look inside the fireball through the products and x-ray the plate in flight. The plate is going very fast (2 km/sec), so the flash x-ray works well in this time frame. It verifies that the plate is flying flat with no spall. The x-ray system used will be the 450 keV system. Two x-ray heads will be used so that the velocity can be determined. The x-ray film and the heads are very close to the exploding cylinder, and therefore protection of the heads and a film packet that can absorb air shock are important. For all of the tests, the distance of 100 mm from the end of the large steel cylinder was the impact point. This was where the plate no longer had the expansion products contributing to it and the plate is flying flat. The first x-ray head is positioned at the 100 mm distance. The test setup is shown in Figures 23 and 24.

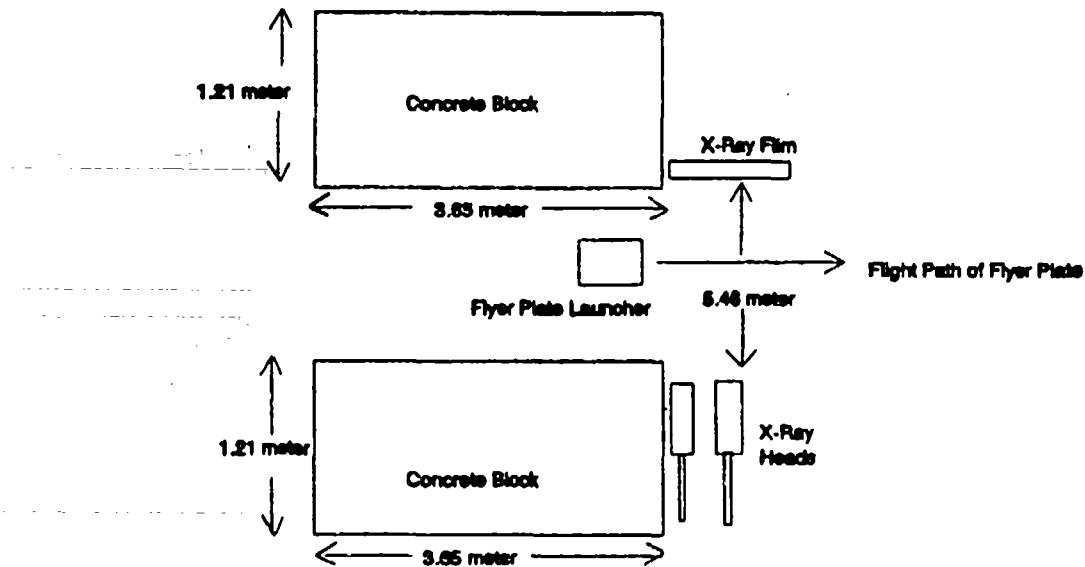


Figure 23. Top View of the Flyer Plate Test Setup



Figure 24. Side View of the Flyer Plate Test Setup

To reduce the overall plate velocity, the length of the explosive used for launching was reduced. With the reduction in length of this charge, a large air gap was used to help reduce the effects from the very curved detonation wave. However, as the air gap was increased, the shock wave in the steel cylinder was given enough time to reach the flyer plate. The shock wave produced a high pressure region around the edges of the flyer plate, which caused it to take the shape of a saucer. Figure 25 is a hydrocode calculation verifying this. Figure 26 is an actual flash radiography of the plate. The solution, as shown in Figures 27 and 28, was to isolate the plate from the cylinder wall using a plexiglass spacer.

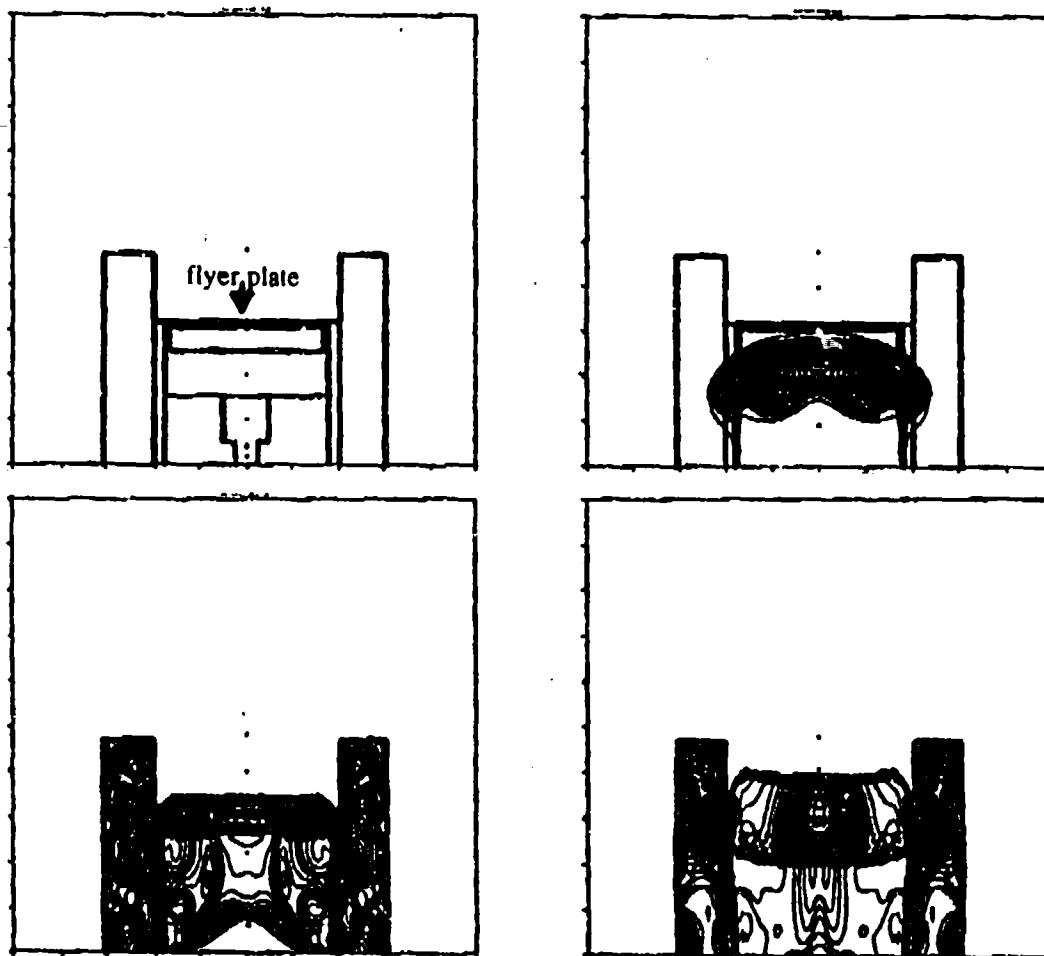


Figure 25. Hydrocode Calculation Predicting High Pressure Region on Edges of Plate

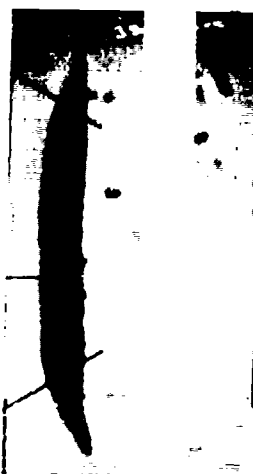


Figure 26. Flash X-Ray of the Flyer Plate Showing High Pressure on Edges of Plate

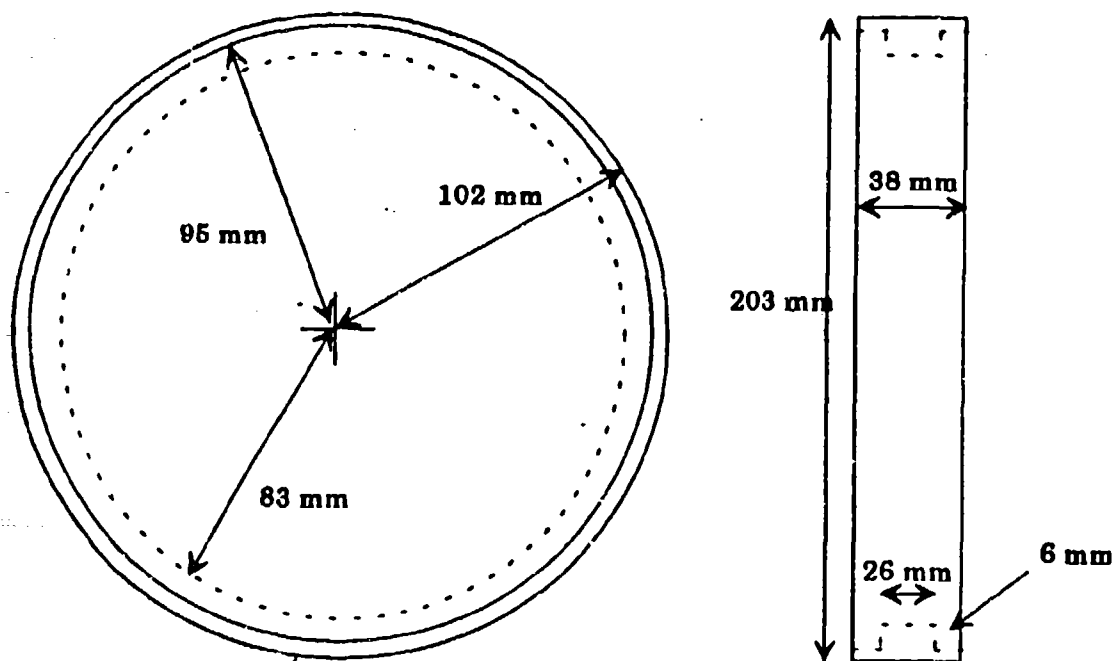


Figure 27. Edge Effects Elimination Device

Figure 28 shows the hydrocode calculation with the steel flyer plate no longer in contact with the steel casewall. Notice the flatness of the flyer plate.

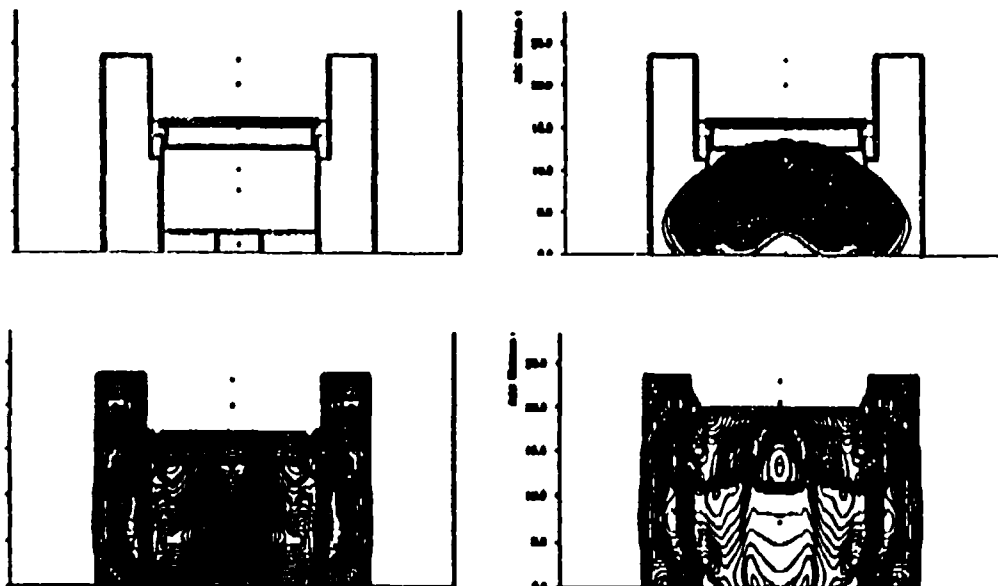


Figure 28. Hull Calculation With Flyer Plate Not in Contact with Steel Cylinder

With this data a new flyer system was developed as shown in Figure 29. The flash x-ray data is shown in Figure 30. This flyer plate is going 2 km/sec.

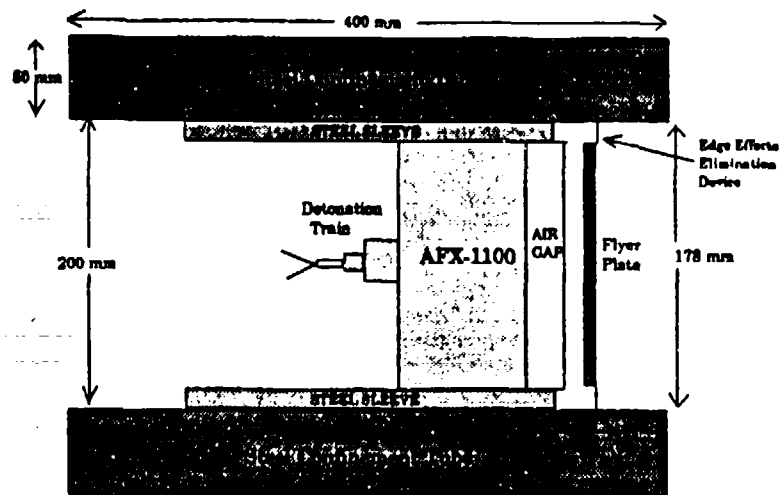


Figure 29. New Flyer Plate Launch System for Low Velocity Plates



Figure 30. Flash X-Ray of Flyer Plate With Uniform Pressure Distribution Across the Back Surface of the Plate

Having solved the problem of reducing flyer plate deformation at various heights, a series of tests was conducted to relate explosive height to plate velocity. Hydrocodes previously conducted had shown the region of interest to be 1-2 km/sec (Figure 31). A calibration curve consisting of four shots is shown in Figure 32.

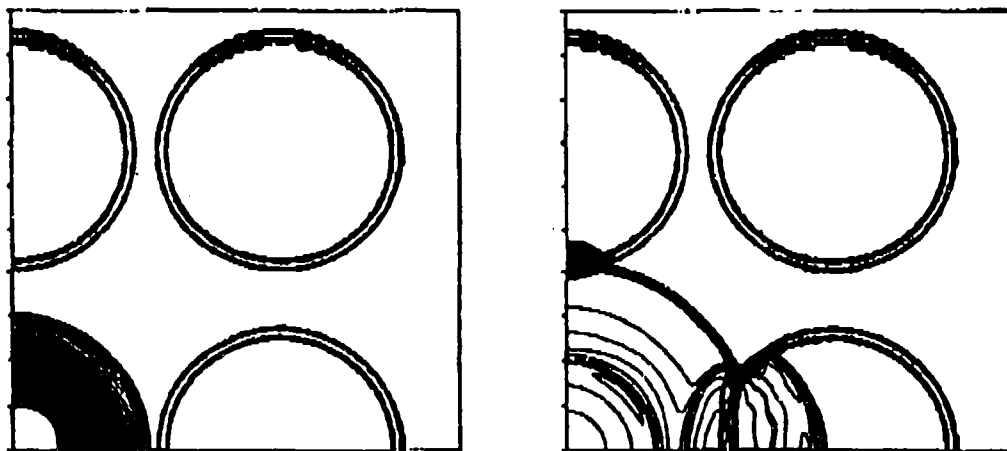


Figure 31. AFX 6441 Calculation of the Detonation of the Donor Bomb With a Flyer Plate Forming at 75 μ s

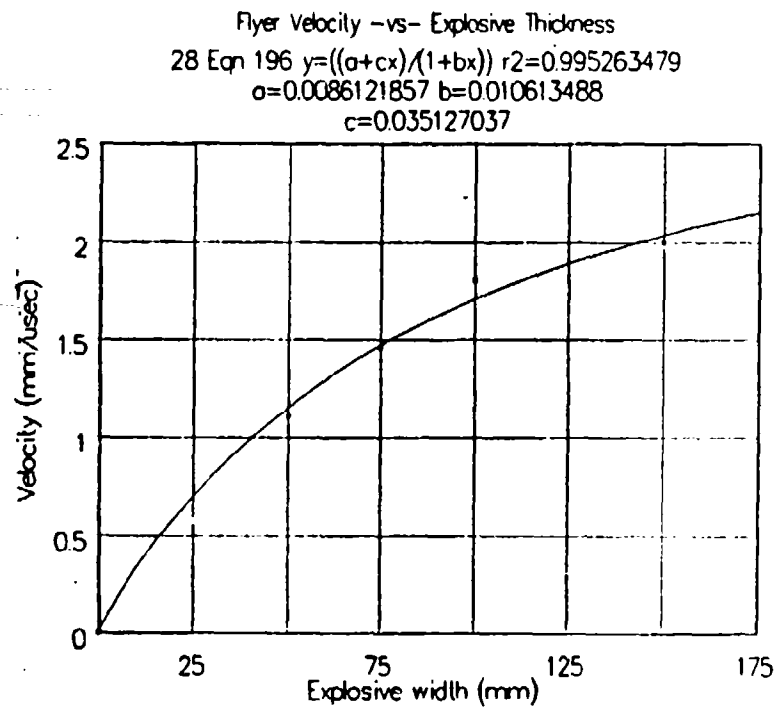


Figure 32. Plot of Flyer Velocity versus Explosive Thickness

The equation that was derived from this plot is shown below.

$$y = ((a + cx)/(1 + bx)) \quad (29)$$

where $r^2 = 0.995$, $a = 0.0086$, $b = 0.0106$, $c = 0.03512$.

SECTION IV

SHOCK TO DETONATION TRANSITION IN CYLINDRICAL CHARGES

With the flyer plate velocity curve established, live acceptors could now be tested using the flyer test. The live acceptors were explosively filled right circular cylinders with piezoelectric pins embedded into the explosive. The cylinders are 1018 cold-rolled steel 250 mm long by 200 mm outside diameter and 180 mm inside diameter. The acceptor cans have 17 pin holes drilled along the long axis and centered on the can. Piezoelectric pins are placed in these holes in a stair-stepped fashion away from the inside surface of the acceptor casewall. A gauge is used to obtain proper spacing of the pins from the casewall. The 17 pins make up two channels of data with the center pin touching the inside surface of the acceptor casewall. A drawing of the setup is shown in Figure 33. Figure 34 is a side view of the test setup; notice the piezoelectric pins embedded in the acceptor cylinder.

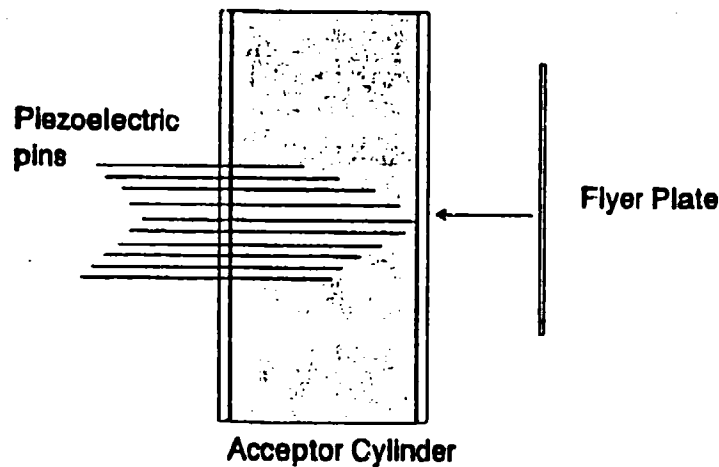


Figure 33. Flyer /Acceptor Setup With Pins in Place

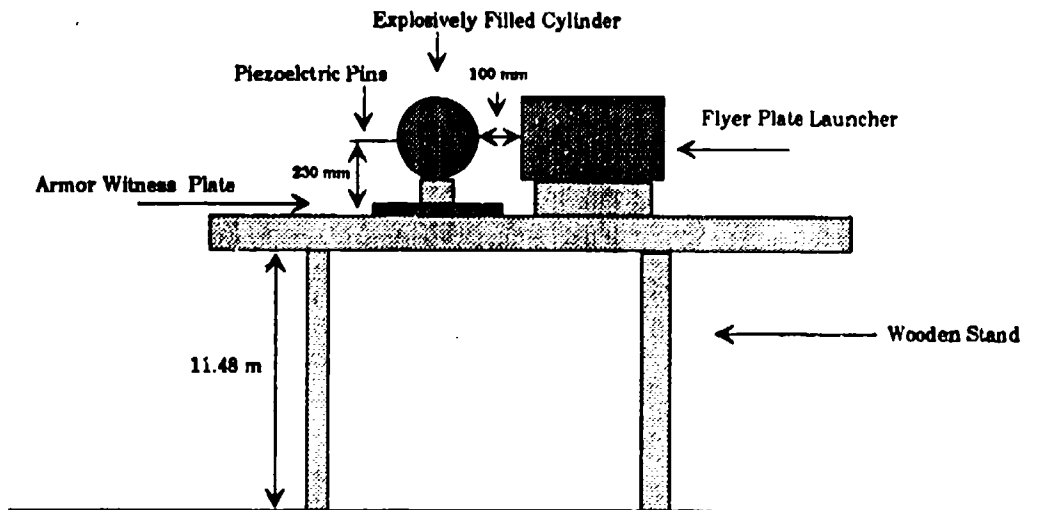


Figure 34. Side View of the Flyer/Acceptor Setup

A second method of obtaining data was the use of a 250 x 250 x 25 mm thick witness plate under the acceptor charge. The armor shows if the acceptor cylinder detonated. If the acceptor does not detonate, the armor will be unmarked. However, this does not mean the acceptor cylinder did not undergo some type of reaction. The other instrumentation gives this kind of detail. Figure 35 is a photograph of the overall test setup.



Figure 35. Overall Test Setup

SECTION V

EXPERIMENTAL RESULTS

Figure 36 depicts the comparison of the simplified model data to the experimental method. The test series utilized an insensitive high explosive (IHE) AFX-6441 in the acceptor charges. The experimental data was gathered using piezoelectric pins. All of the data was fitted. The IHE used in the acceptor exhibited a go-no-go point at a pressure of approximately 70 kbars, which corresponds to a shock velocity of 4.04 mm/ μ s, which results in a detonation. The run-up equation derived from ELSGT tests is $\log X^* = -3.24 \log P^* + 5.21$. A shock velocity of 4.2 mm/ μ s corresponds to a pressure of 81 kbars, which results in a run of 185 mm. The detonation velocity of this explosive is 7.1 mm/ μ s. From Figure 36, by 120 mm the transition to detonation is almost complete. The implication is that the induced pressure is actually higher or the pop plot is in error. The model predicts a detonation for the 1.9 mm/ μ s flyer against this explosive using a 12.7 mm critical diameter and no detonation at 1.48 mm/ μ s. Interface shock velocities predicted by the model are approximately 4 percent higher in all cases.

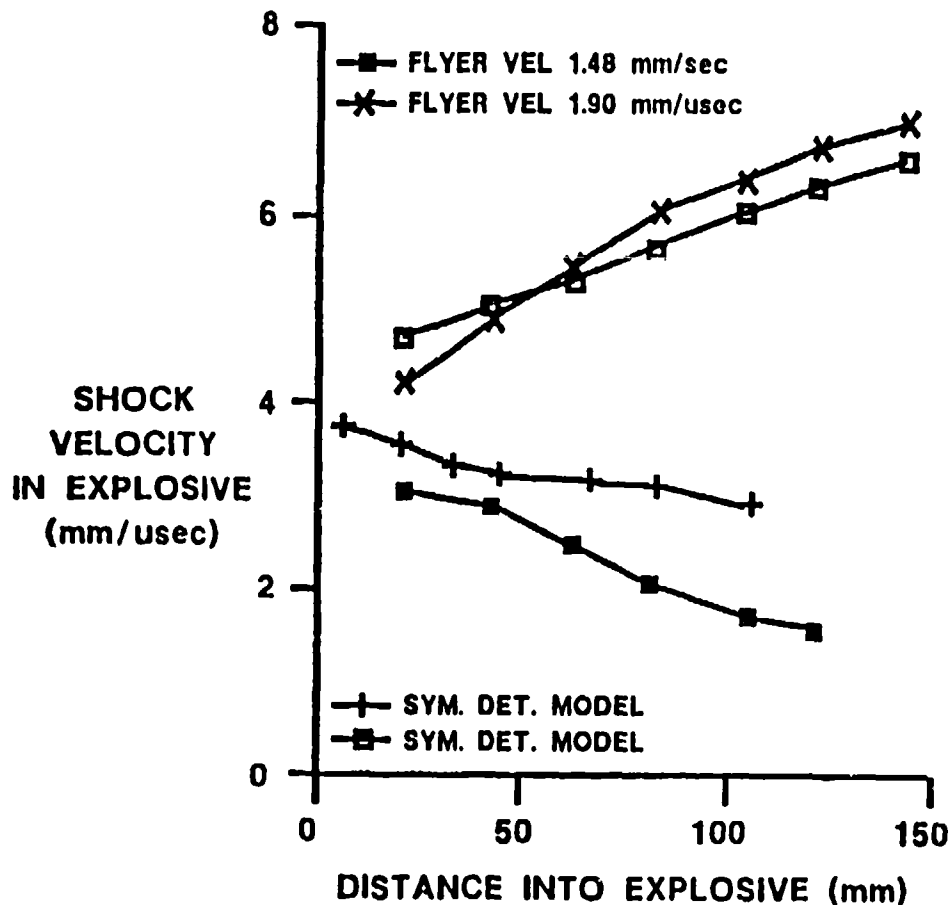


Figure 36. Comparison of the Simplified Model With the Experimental Data

Figure 37 is the manganin stress data for the 1.9 mm/ μ s flyer velocity. The predicted pressure at this point (13 mm into the explosive) was 55 kbars. The constantan strain gauge revealed that the manganin gauge started receiving a non-planar stress wave approximately 100 nanoseconds into the event. It is believed that the true peak pressure signal was lost due to this problem. The technique is still being perfected, and more tests will be performed to obtain the actual pressure.

The pulse duration for this test as shown in Figure 37 is given as 0.986 μ s. This compares TOA predicted pulse duration of 1.07 μ s. It is not known the exact effect the non-planar wave has on pulse duration.

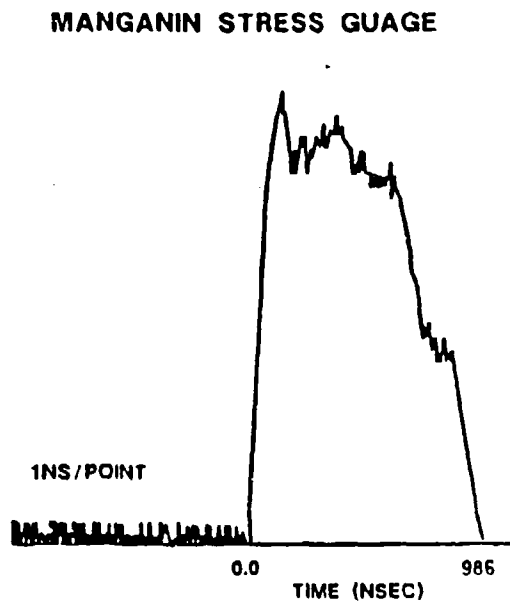


Figure 37. Manganin Gauge Data

SECTION VI

DISCUSSION AND CONCLUSIONS

The purpose of this research effort was to develop a means of predicting the likelihood of sympathetic detonation in the storage configuration for explosive fills under development. Since it is not clear which mechanism or combination of mechanisms is responsible for sympathetic detonation (these may vary from explosive to explosive), the goal was to develop a test that accurately reproduces the conditions observed in the storage configuration. If the boundary conditions can be reproduced, then those mechanisms should exhibit themselves. While it is possible to instrument rounds in the storage configuration, this experiment allows much greater control of the acceptor environment.

Results of the model indicate interface pressures approximately 12 percent above those recorded in the experiment. However, at 12.7 mm, the calculated pressure for the 1.9 mm/ μ s impact test is 83 kbars or 2 percent above the experimental result. Assuming the runup was induced by the calculated interface pressure of 93 kbar, the predicted runup is 118 mm, significantly closer to that observed in the experiment than would be predicted by an 81 kbar initiation. The model, as mentioned previously, predicts sufficient stimulus to achieve detonation. Only the physical size of the acceptor charge prevents this. This suggests the interface values predicted by the model are reasonably accurate but the rate of shock wave decay may be too low. The calculated pressures at 12.7 mm into the explosive for the 1.48 mm/ μ s impact point is 51 kbar. The one-dimensional region in the explosive varies but was generally controlled by lateral relief.

Differences between the model and the experiment may be due to curvature in the impacting plate, small errors in impact velocity, or differences in the Hugoniot modeled and that tested. Regardless, the model predicts with a high degree of accuracy the interface condition in the round-to-round acceptor experiment, giving the explosives formulator a quick and accessible tool to determine the likelihood of sympathetic detonation. Similarly, the flyer plate test has proven to be a versatile and valuable tool in assessing safety margins or lack thereof of rounds in the storage configuration.

REFERENCES

1. J.G. Glenn, M.E. Gunger, and H.C. McCormick, *Sympathetic Detonation Predictive Methods*, WL/MN-TR-93-7001, Eglin AFB FL 32542-5434.
2. P.J. Miller, *Determining JWL Equation of State Parameters Using the Gurney Approximation*, 9th Symposium on Detonation, paper 203, August 1989.
3. E.N. Ferm, J.B. Ramsey, *Spherical Projectile Impact on Explosives*, 9th Symposium on Detonation, paper 41, August 1989.
4. A.C. Victor, *Simple Analytical Relationships for Munitions Hazard Assessment*, DDESB Explosives Safety Seminar, August 1992.
5. L. Green, *Shock Initiation of Explosives by Impact of Small Diameter Cylindrical Projectiles*, 7th Symposium on Detonation, pg. 273-277, June 1981.
6. R.A. Benham, and W.R. Kampfe, *Ultra-High Velocity Impacts Utilizing a Rocket Sled and an Explosively Accelerated Flyer Plate*, Shock and Vibration Bulletin, No. 55, Pt. 2, June 1985, page 51-56.

**DISTRIBUTION
(WL-TR-93-7030)**

**Defense Technical Information Center
Attn: DTIC-DDAC
Cameron Station
Alexandria VA 22304-6145
1**

**WLMNOI (STINFO Facility)
203 W. Eglin Blvd., Ste 300
Eglin AFB FL 32542-6843
1**

**WLMNME (J. Gregory Glenn)
101 W. Eglin Blvd., Ste 219
Eglin AFB FL 32542-6810
4**

**AFDTC/PA
101 W. D Avenue, Ste 129
Eglin AFB FL 32542-5498
1**

SUPPLEMENTARY

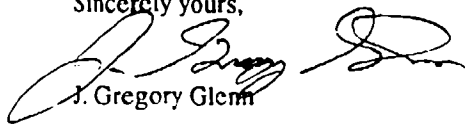
INFORMATION

30 Sept. 93

To whom it may concern,

Greetings, my name is J. Gregory Glenn, you have recently received a report titled Simulating Sympathetic Detonation Effects (Report # WL-TR-93-7030). In my hurry to finish the report I left out a very important part. The part that I am referring to is the acknowledgments located on page iii. I am sending the proper acknowledgments and am asking you to please replace this with the one in the report. I would fill remiss if I did not acknowledge the help that I received from these people. Thank you for your help in this matter.

Sincerely yours,


J. Gregory Glenn

CRBATA ADA 220 387

PREFACE

This in house was prepared by WL/MNME, Eglin Air Force Base Florida 32542-6810 performed during the period from April 1991 to April 1993. J. Gregory Glenn managed the program for the Wright Laboratory. The authors are thankful for the following individual contributions:

- a. Messrs Gary Parsons and Larry Pitts provided valuable advice, direction and encouragement.
- b. The High Explosives Research and Development (HERD) Facility Processing Laboratory personnel under the supervision of Mr. Arthur Spencer fabricated and loaded all explosive charges.
- c. The Armament Laboratory Model Shop under the supervision of Mr. Lonnie B. English fabricated all hardware that was used for this program.